Optical reset modulation in the SiO_2/Cu conductive-bridge resistive memory stack

T. Kawashima,[1,2,a)] Y. Zhou,[1] K. S. Yew,[1] and D. S. Ang[1,b)]
[1]*School of Electrical and Electronic Engineering, Nanyang Technological University, Singapore 639798, Singapore*
[2]*Toshiba Corporation, 33, Shin-Isogo-Cho, Isogo-ku, Yokohama 235-0017, Japan*

(Received 15 May 2017; accepted 2 September 2017; published online 15 September 2017)

We show that the negative photoconductivity property of the nanoscale filamentary breakdown path in the SiO_2 electrolyte of the SiO_2/Cu conductive bridge resistive random access memory (CBRAM) stack is affected by the number of positive-voltage sweeps applied to the Cu electrode (with respect to a non-metal counter electrode). The path's photo-response to white light, of a given intensity, is *suppressed* with an increasing number of applied positive-voltage sweeps. When this occurs, the path may only be disrupted by the light of a higher intensity. It is further shown that the loss of the path's photosensitivity to the light of a given intensity can be recovered using a negative-voltage sweep (which eliminates the path), followed by the reformation of the path by a positive-voltage sweep. The above behavior is, however, not seen in the SiO_2/Si stack (which involves a non-metal Si electrode), suggesting that the photo-response modulation effect is related to the Cu electrode. The demonstrated reversible electrical modulation of the path's photo-response may afford greater flexibility in the electro-optical control of the CBRAM device. *Published by AIP Publishing.* [http://dx.doi.org/10.1063/1.5003107]

Alternative memory concepts, such as phase change,[1,2] spin-torque transfer,[3] and resistance switching[4–16] have been pursued as possible solutions for overcoming the scaling limitations of the flash memory and dynamic random access memory. The resistive memory is a promising candidate for a universal memory due to its outstanding properties, such as simple metal-insulator-metal stack structure, nanoseconds switching time, large on/off ratio, low-energy consumption, high endurance and scalability.[6–16] In particular, the SiO_2/Cu conductive-bridge random access memory (CBRAM) has garnered considerable attention, as its compatibility with the backend interconnect technology raises significantly the prospect of a faster route to a fully embedded memory solution.[6,10] Resistance switching in Cu CBRAM is enabled by electric-field-driven formation/dissolution of microscopic Cu filaments inside the oxide electrolyte.[17,18] The physical evidence of field-induced Cu-ion migration in the oxide electrolyte has been reported.[19–21]

We have recently shown that white light could "disrupt" the filamentary breakdown path, formed in a wide-bandgap oxide (e.g., HfO_2, SiO_2, ZrO_2) during an electrical soft-breakdown (SBD) process.[22–25] The effect, named light-induced reset or negative photoconductivity (NPC), is manifested as a decrease of the conduction current or increase of the breakdown oxide resistance upon light exposure, akin to the electrical reset in a resistive memory device. By adjusting the light intensity and exposure dose, different rates of current decrease and conductance states may be achieved.[22] The findings raise the prospect of engaging these otherwise non-photo-responsive wide-bandgap oxides for optical applications, expanding the functionality of electrical systems based on these oxide materials.

In this paper, we present a detailed study on the NPC response of the filamentary breakdown path in the SiO_2/Cu stack. An intriguing behavior, whereby the photosensitivity of the path may be modulated by a positive voltage applied to the Cu electrode (with respect to a non-metal counter electrode), is revealed. Specifically, the repeated application of a positive voltage to the Cu electrode can cause the path to lose its NPC response. The loss in NPC response may be restored using a negative voltage (which leads to an electrical reset similar to that in a SiO_2/Cu CBRAM device), followed by the reformation of the breakdown path by SBD again. Such an NPC modulation effect is, however, not seen in the SiO_2/Si stack, lending support to a proposed role of the Cu electrode behind the observation. While the exact mechanism requires further confirmation, our demonstration of NPC-sensitivity tuning of the filamentary breakdown path in the SiO_2/Cu stack by a straightforward electrical means indicates a possibility of engaging the CBRAM as an electro-opto device.

On an hydrogen fluoride-cleaned p-type Si(100) substrate (of resistivity $5 \times 10^{-3} - 1 \times 10^{-2}\,\Omega\,\mathrm{cm}$), a 30-nm Ti adhesion layer followed by a 30-nm Cu electrode were deposited by DC magnetron sputtering. Subsequently, a 10-nm SiO_2 layer was grown at 250 °C via a parallel-plate plasma-enhanced chemical vapor deposition process using SiH_4 and N_2O gases to form the SiO_2/Cu stack. No top electrode deposition was carried out. For comparison, a SiO_2(5-nm)/p-Si stack was also fabricated; the SiO_2 thickness was reduced to keep the breakdown voltage at a moderate level [cf. Fig. 2(b)]. After the SiO_2 growth, the samples were loaded into an ultra-high vacuum ($\sim 5 \times 10^{-10}$ Torr) conductive atomic force microscopy (C-AFM) system. A diamond-coated Si cantilever probe functioned as the top non-metal

a)E-mail: tomohito.kawashima@toshiba.co.jp
b)Author to whom correspondence should be addressed: edsang@ntu.edu.sg

electrode, simulating a nanoscale CBRAM device or transistor gate stack (Fig. 1). The breakdown of the SiO_2 was made using a voltage sweep supplied by a parameter analyzer to the probe while the bottom Cu or Si electrode was grounded. A current compliance (1.1 nA) setting prevented progression towards hard breakdown. The vacuum environment helped avoid surface contamination and anodic oxidation. An light-emitting diode (LED) lamp, having constituent wavelengths of 400–700 nm, positioned at a quartz window of the C-AFM system served as the white light source. No heating of the sample by the LED lamp was found even after an extended illumination period.[23]

Typical current-voltage (*I–V*) curves of the SBD step (A) and subsequent voltage-sweep measurements are depicted in Figs. 2(a) and 2(b), respectively, for the SiO_2/Cu and SiO_2/Si stacks. Abrupt increase in the current to the compliance level marks the formation of a filamentary breakdown path in the SiO_2. Despite the 2× thicker SiO_2, the breakdown voltage (at which the current-jump occurs) of the SiO_2/Cu stack is about half that of the SiO_2/Si stack. The lower breakdown voltage may be attributed to the migration of Cu ions into the SiO_2, driven by the negative-voltage sweep of the SBD step. Studies on Cu CBRAM[19–21] have found that under a large oxide field, Cu ions from the electrode may migrate into the oxide, resulting in the formation of a Cu filament. The presence of Cu ions in the SiO_2 at the probe location increases the electric field there, due to a decrease of the effective oxide thickness. This is believed to have facilitated the dissociation of Si-O bonds and the breakdown of the SiO_2 at a lower voltage than in the SiO_2/Si stack. A study that used atomic-scale spectroscopy[26] has found an oxygen-deficient or vacancy-populated breakdown oxide region, implying that the Si-O bond dissociation and field- and thermal-induced migration of the released oxygen ions away from the dissociated bonds result in the SiO_2 breakdown.

During the post-breakdown positive-voltage sweep (B) of the SiO_2/Si stack, no decrease in the current can be seen [Fig. 2(a)], indicating that breakdown recovery did not occur. This is apparent from the following negative-voltage sweep (C), which produced an *I–V* curve similar to curve A in the reverse sweep direction. The absence of breakdown recovery was obtained on 29 other breakdown locations on the SiO_2/Si stack. This observation draws similarity to the lack of breakdown recovery in the polysilicon/HfO_2/Si stack.[27] In contrast, breakdown recovery can be readily observed in the TiN/HfO_2/Si stack by negatively biasing the TiN. The

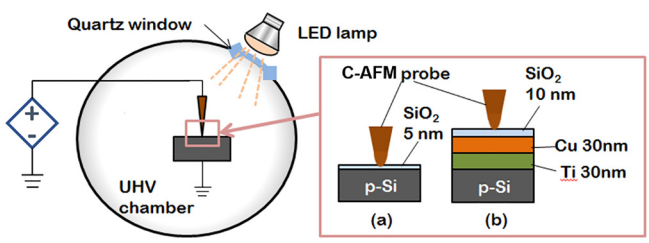

FIG. 1. Schematic illustration of the ultra-high vacuum (UHV) conductive atomic force microscopy (C-AFM) setup and the two test samples (not drawn to scale) used in this study. The C-AFM probe is connected to a source/monitor unit of a semiconductor parameter analyzer. White-light illumination is provided by an LED lamp, positioned at a quartz window of the UHV chamber, ~30 cm away from the test sample.

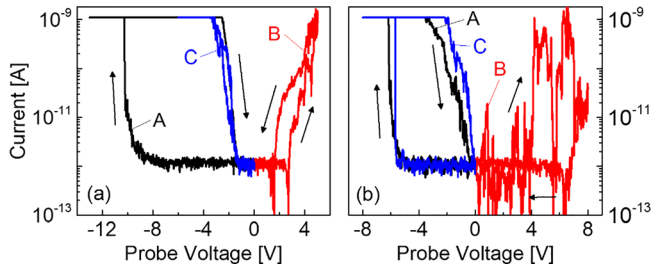

FIG. 2. Current-voltage (*I-V*) curves of (a) SiO_2/p-Si and (b) SiO_2/Cu/Ti/p-Si stacks. A negative-voltage ramp (curve A, black) for initiating SiO_2 breakdown was applied, followed by a positive-voltage ramp (curve B, red) and then a negative-voltage ramp (curve C, blue). Arrows indicate the directions of voltage sweeps.

difference has been ascribed to the migration of oxygen ions from the TiN interface region into the breakdown path. Resultant recombination with the vacancy defects leads to the disruption of the path. However, such a supply of oxygen ions is deemed lacking in the polysilicon/HfO_2/Si stack due to the stronger Si-O bonds. The dissociation energy of the Si-O bond is 8.29 eV, larger than that of the Ti-O bond (6.91 eV).[28] This makes the dissociation of Si-O bonds more difficult, hence limiting the supply of oxygen from the Si interface region. Oxygen ions driven towards the Si substrate during the breakdown may also be "locked-in" by the formation of Si-O bonds, thus restricting their drift back to the breakdown path during the positive-voltage sweep. It should be mentioned that a further breakdown of the SiO_2 occurs when the positive-voltage sweep is extended.[23]

On the other hand, an obvious decrease in the current can be seen for the SiO_2/Cu stack [Fig. 2(b)], indicating that breakdown recovery occurred during the positive-voltage sweep (B). The recovery is near-complete, as is evidenced by the ensuing negative-voltage sweep (C) which yielded an *I–V* curve like the pre-breakdown case. More than 80% of the 30 breakdown locations on the SiO_2/Cu stack exhibit near-complete recovery; the remaining show partial recovery. This easy occurrence of breakdown recovery may be attributed to (1) the migration of Cu ions in the breakdown path to back to the electrode under a reverse electric field[17–21] and (2) the availability of oxygen ions from the Cu interface region for reducing the vacancy defects in the breakdown path. The dissociation energy of the Cu-O bond is 2.98 eV,[28] much smaller than those of the Ti-O and Si-O bonds. Thus, oxygen ions from the Cu cathode region may readily migrate to the breakdown path, just like in the HfO_2/TiN.[22,27] To check the above explanation, breakdown of the SiO_2/Cu stack was also induced by a positive-voltage sweep, opposite to the previous case. Compared to the negative-voltage sweep, the breakdown voltage is increased, since Cu-ion migration into the oxide was prevented. In accordance to the above explanations, the breakdown path did not display electrical reset during negative-voltage sweeping, (1) because this voltage polarity prevented the migration of oxygen ions from the Cu interface region into the breakdown path and (2) because of a lack of oxygen migration from the exposed probe/oxide interface which failed to retain oxygen ions released during the SBD step.

Figure 3(a) depicts the response of the breakdown path in the SiO_2/Cu and SiO_2/Si stacks to white-light illumination. The light intensity at the test sample surface was

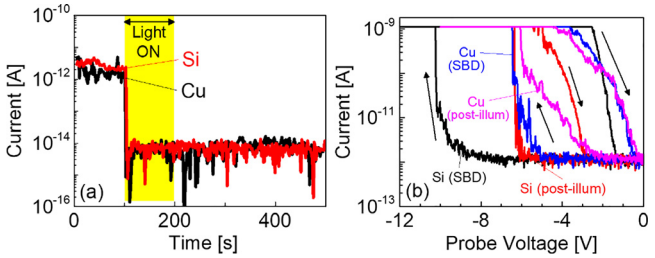

FIG. 3. (a) Current-time (*I-t*) plots of the SiO_2/p-Si (Si) and SiO_2/Cu/Ti/p-Si (Cu) stacks showing the disruption of the breakdown path under white-light illumination. A low voltage of –1.5 V and –1 V, respectively, was applied to the C-AFM probe for sensing the breakdown current. The currents in both stacks show a steep decrease upon illumination at 100 s and remain low at $\sim 10^{-14}$ A after the light was turned off at 200 s. (b) Comparison of the forward and reverse-sweep current-voltage curves for the first soft-breakdown (SBD) step and the re-breakdown step after illumination (post-illum).

$\sim 2\,mW/cm^2$, determined from a separate measurement using a solar meter positioned roughly at the same distance from the light source as the test sample. In the 100-s period before illumination, a constant current was recorded at the monitoring voltage of –1 V, indicating that the breakdown path and the C-AFM probe were stable. Upon illumination at 100 s, a significant decrease of the breakdown current, from $\sim 10^{-12}$ to $\sim 10^{-14}$ A (measurement floor), can be observed in both cases, similar to the NPC response of the HfO_2/TiN stack.[22] A negative-voltage sweep applied after the illumination produced *I–V* curves that are partially shifted back towards the respective pre-breakdown curves [Fig. 3(b)], indicating that some degree of photo-induced recovery of the breakdown paths has occurred.[23] By alternating between electrical SBD and light exposure, the breakdown path in both stacks can be repeatedly switched between the electrical set (low resistance) and optical reset (high resistance) states, respectively. With our present set-up, the number of switching cycles is limited (~70) due to the thermal drift of the C-AFM probe.

It has been proposed[23] that the optical reset proceeded with the photo-excitation of interstitial oxygen ions surrounding the breakdown path, resulting in their migration and recombination with the vacancy defects in the path. Besides the electric-field directed migration of oxygen ions (released from the Si-O bond dissociation during the breakdown process) towards the anode, these oxygen ions may also propagate laterally outwards from the breakdown site due to Joule heating, and some of them remained in the proximity when the process is aborted.[29] The migration barrier for interstitial oxygen ions within the oxide network is ~0.11–0.27 eV,[30] which corresponds to $\sim 1.8\text{–}4.3 \times 10^{-20}$ J. Considering that the light intensity at the oxide surface is 2 mW/cm^2 or 2×10^{-19} J/s·Å^2, it is plausible for photo-induced migration of interstitial oxygen ions to occur, resulting in the disruption of the breakdown path. In contrast, such reverse migration of surrounding interstitial oxygen ions to the breakdown site would not occur during voltage sweeping, as Joule heating would tend to favor the outward propagation of these ions instead. Thus, breakdown recovery could not occur in the SiO_2/Si stack during the voltage sweep [Fig. 2(a)].

Here, we also discuss the quasi-conduction band (QCB) model,[31] which appears consistent with the optical reset but not with the electrical reset observations. First-principles simulation (e.g., Ref. 32) has revealed a defect band, attributed to oxygen vacancies, situated ~2 eV below the SiO_2 conduction band edge. When filled by the electron flux during breakdown, this defect band may be coupled to the electrodes to form a QCB throughout the system, giving rise to the persistent low-resistance state after SBD. Under illumination by white light (having photon energy from ~1.8 to 3.1 eV), the photoexcitation of the trapped electrons to the conduction band occurs. Consequently, the defect band is decoupled from the electrodes and the QCB is annihilated, causing a transition to the high-resistance state. A similar decoupling may occur when the trapped electrons are depopulated via tunneling to the conduction band under a sufficiently large voltage bias, triggering an electrical reset.[31] However, a major discrepancy is surfaced here since electrical reset is observed only in the SiO_2/Cu stack but not in the SiO_2/Si stack. Difference in the SBD I-V curves of the two stacks (Fig. 2) falls well within the distribution obtained on a given stack [Fig. 4(c)]. In this absence of major deviation, the complete lack of the electrical reset in the SiO_2/Si stack is "puzzling" in the context of the QCB model. On the other hand, the model on the migration of oxygen (the lack of which in the SiO_2/Si stack) may address the discrepancy satisfactorily and consistently explain the optical and electrical reset (or the lack of) in our samples.

The electrical modulation of the optical reset in the SiO_2/Cu stack is demonstrated in Fig. 4. SBD was first induced by a negative-voltage sweep (0 → –8 V at 1.1 nA compliance) applied to the C-AFM probe. The breakdown path was then checked for an NPC response or further subjected to a varying number of the same negative-voltage sweeps before illumination was applied. The procedure was repeated on numerous randomly selected locations on the test sample. It should be noted that positive-voltage sweeping was not applied as this would disrupt the breakdown path and cause a reset electrically, as shown in Fig. 2(b).

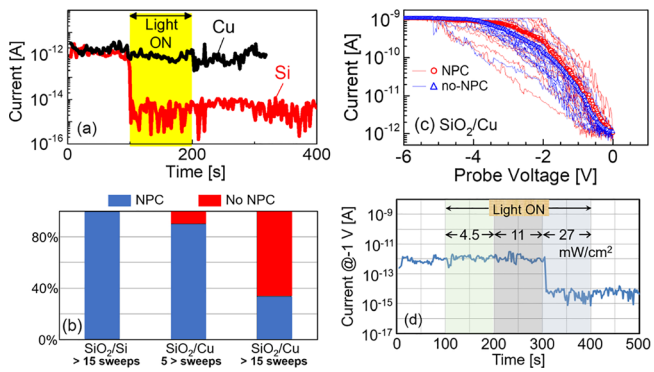

FIG. 4. (a) Current-time (*I-t*) plots depicting the effect of white-light illumination on the breakdown path in the SiO_2/p-Si (Si) and SiO_2/Cu/Ti/p-Si (Cu) stacks, after subjecting each path to more than 15 negative-voltage sweeps. (b) The percentage of breakdown paths (out of a total of 30 each) which can still display the NPC behavior after a certain number of negative-voltage sweeps. (c) Pre-illumination current-voltage (*I-V*) curves of 20 breakdown paths which show NPC behavior (thin red lines) and those of 20 other breakdown paths which lost their NPC behavior after more than 15 negative-voltage sweeps (thin blue lines). The respective averaged I-V curves are also shown (symbols). (d) After numerous negative-voltage sweeps, a breakdown path can only be disrupted by a much higher light intensity.

For breakdown paths that were subjected to only a few (< 5) negative-voltage sweeps (including the SBD step), a majority (~80%) of them display the NPC response during illumination, as shown in Fig. 3(a). In contrast, only a minority (~30%) of the breakdown paths could show the NPC response after being subjected to 15 negative-voltage sweeps prior to the illumination. The majority failed to register any NPC response, i.e., the current is unperturbed during illumination [Fig. 4(a)]. The observations indicate that the NPC response of the breakdown path in the SiO_2/Cu stack can be manipulated by the number of times the Cu electrode is positively biased with respect to the non-metal counter electrode (C-AFM probe).

However, the same procedure, when applied on the SiO_2/Si stack, did not impact the NPC response of the breakdown path. After more than 15 negative-voltage sweeps, the breakdown path can still be disrupted upon illumination [Fig. 4(a)], with no apparent difference from the case without any additional voltage sweeps applied [Fig. 3(a)]. A study on 30 random breakdown locations shows that all of them retain their NPC response after more than 15 sweeps. This shows that the NPC modulation effect seen in the SiO_2/Cu stack is linked to the Cu electrode.

Next, we examine two scenarios which may have led to the breakdown path in the SiO_2/Cu stack losing its NPC response after repeated negative-voltage sweeps. First, Joule heating during voltage sweeping may cause a progression towards more severe breakdown, due to further dissociation of weak Si-O bonds within the breakdown region and propagation of the released oxygen ions further away from the breakdown path.[29] Consequently, the path may become less responsive to illumination because of the reduced availability of interstitial oxygen in its proximity.[22] This effect is intrinsic and thus should be common to both stacks. Its relevance to the SiO_2/Cu stack is, however, not supported since repeated voltage sweeping has no impact on the NPC response of the breakdown path in the SiO_2/Si stack. Moreover, transition to a more severe breakdown after repeated voltage sweeping should be accompanied by a change in the I-V curve. This is not borne out by a comparison made between the pre-illumination *I–V* curves of 20 breakdown locations which were NPC responsive immediately after breakdown and those of 20 other locations which lost their NPC response after 15 repeated voltage sweeps [Fig. 4(c)]. As can be seen, the two sets of I-V curves are closely overlapped and the averaged I-V curves are not statistically different.

The second scenario is depicted in Fig. 5. It is reported that Cu ions could precipitate in a solid electrolyte[33] (SiO_2 in our case), with gaps in between the Cu-ion clusters. After SBD, the breakdown path may be made up of both Cu-ion and vacancy clusters [Fig. 5(a)]. The existence of vacancies in the path makes it NPC responsive, as photon-stimulated migration of oxygen ions in the path's vicinity and their recombination with the vacancies in the path would disrupt it, leading to a partial restoration of the oxide resistance[22] [Fig. 3(b)]. If a negative-voltage sweep is repeatedly applied after breakdown, more Cu ions would be drawn into the path,[17] occupying the vacancies there to form a complete Cu filament [Fig. 5(b)]. First-principles calculation[34] has shown that metal-ion migration in an oxide network is enhanced by

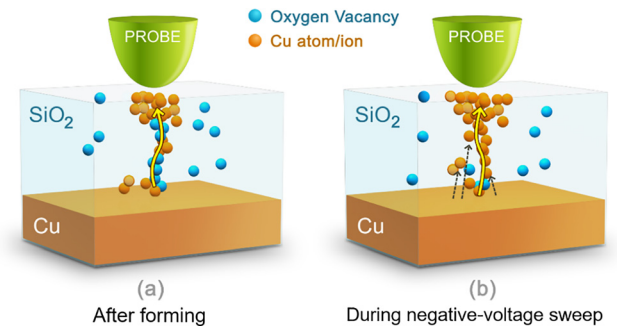

FIG. 5. Schematic diagrams showing (a) the initial state of a breakdown path in the SiO_2/Cu/Ti/p-Si stack after breakdown; (b) change in the path composition after numerous negative-voltage sweeps applied to the C-AFM probe. Cu ions drawn from the bottom Cu electrode into the breakdown region by the negative-voltage sweep (see dotted arrows) fill the oxygen vacancies present there, resulting in the formation of a complete Cu filament.

the presence of vacancies. The disruption of the Cu filament requires not only the cleavage of Cu-Cu bonds but also the ionization of Cu to Cu^+ or Cu^{2+}. The Cu-Cu bonding energy is 2.08 eV (Ref. 28) and the first ionization energy to form Cu^+ is 7.73 eV,[35] requiring a total energy of 1.57×10^{-18} J, ~10× larger than the energy provided by the 2 mW/cm^2 light source. Thus, the light is unable to disrupt the breakdown path in the SiO_2/Cu stack after a complete Cu filament is formed. A change in vacancy distribution has been shown to significantly impact the magnetic and electrical properties of $SrTiO_3$.[36,37] In our case, the lack of a discernable change in the I-V curve after complete Cu filament formation needs further study [Fig. 4(c)].

To check the above hypothesis, a breakdown path was generated using a negative-voltage sweep on a randomly selected position on the SiO_2/Cu stack. The path registered the NPC response when illuminated by the white light of intensity 4.5 mW/cm^2. After the illumination, the breakdown path was reformed using a negative-voltage sweep. This was followed by more than 15 negative-voltage sweeps before the path was subjected to the white light of the same intensity. The path now failed to show any NPC response [Fig. 4(d)]. The same breakdown path was then subjected to the white light of successively higher intensity (11 and 27 mW/cm^2). Interestingly, an NPC response was recorded under the strongest illumination [having intensity >10× of that used in Fig. 4(a)], lending support to the above hypothesis.

Experimental results have shown that the NPC response of the breakdown path in the SiO_2/Cu stack can be suppressed by multiple negative-voltage sweeps applied to the non-metal counter electrode (or positive-voltage sweeps applied to the Cu electrode). However, such an effect is not observed in the SiO_2/Si stack, where a non-metal Si electrode is used, pointing to a definite role by the Cu electrode in the observed NPC response modulation. A hypothesis involving Cu ions migration, due to the applied voltage sweeping, into the breakdown path and occupying the vacancy defects there to form a Cu filament is proposed. Consequently, the photo-induced oxygen-vacancy recombination (believed to have given rise to the NPC response) is suppressed and thus the NPC response is affected. Preliminary calculations have indicated that a stronger light intensity is needed to disrupt a Cu filament which has been supported experimentally.

[1]F. Xiong, E. Yalon, A. Behnam, C. M. Neumann, K. L. Grosse, S. Deshmukh, and E. Pop, in *International Electron Devices Meeting, Technical Digest* (2016), p. 4.1.1.
[2]S. Raoux, W. Wełnic, and D. Ielmini, Chem. Rev. **110**, 240 (2010).
[3]S.-W. Chung, T. Kishi, J. W. Park, M. Yoshikawa, K. S. Park, T. Nagase, K. Sunouchi, H. Kanaya, G. C. Kim, K. Noma, M. S. Lee, A. Yamamoto, K. M. Rho, K. Tsuchida, S. J. Chung, J. Y. Yi, H. S. Kim, Y. S. Chun, H. Oyamatsu, and S. J. Hong, in *International Electron Devices Meeting, Technical Digest* (2016), p. 27.1.1.
[4]J. Y. Seok, S. J. Song, J. H. Yoon, K. J. Yoon, T. H. Park, D. E. Kwon, H. Lim, G. H. Kim, D. S. Jeong, and C. S. Hwang, Adv. Funct. Mater. **24**, 5316 (2014).
[5]J. H. Yoon, K. M. Kim, S. J. Song, J. Y. Seok, K. J. Yoon, D. E. Kwon, T. H. Park, Y. J. Kwon, X. Shao, and C. S. Hwang, Adv. Mater. **27**, 3811 (2015).
[6]J. Zahurak, K. Miyata, M. Fischer, M. Balakrishnan, S. Chhajed, D. Wells, H. Li, A. Torsi, J. Lim, M. Korber, K. Nakazawa, S. Mayuzumi, M. Honda, S. Sills, S. Yasuda, A. Calderoni, B. Cook, G. Damarla, H. Tran, B. Wang, C. Cardon, K. Karda, J. Okuno, A. Johnson, T. Kunihiro, J. Sumino, M. Tsukamoto, K. Aratani, N. Ramaswamy, W. Otsuka, and K. Prall, in *International Electron Devices Meeting, Technical Digest* (2014), p. 6.2.1.
[7]A. Bricalli, E. Ambrosi, M. Laudato, M. Maestro, R. Rodriguez, and D. Ielmini, in *International Electron Devices Meeting, Technical Digest* (2016), p. 4.3.1.
[8]J. R. Jameson, P. Blanchard, C. Cheng, J. Dinh, A. Gallo, V. Gopalakrishnan, C. Gopalan, B. Guichet, S. Hsu, D. Kamalanathan, D. Kim, F. Koushan, M. Kwan, K. Law, D. Lewis, Y. Ma, V. McCaffrey, S. Park, S. Puthenthermadam, E. Runnion, J. Sanchez, J. Shields, K. Tsai, A. Tysdal, D. Wang, R. Williams, M. N. Kozicki, J. Wang, V. Gopinath, S. Hollmer, and M. Van Buskirk, in *International Electron Devices Meeting, Technical Digest* (2013), p. 30.1.1.
[9]X. Xu, Q. Luo, T. Gong, H. Lv, S. Long, Q. Liu, S. S. Chung, J. Li, and M. Liu, in IEEE Symposium VLSI Technology (2016).
[10]L. Goux, A. Belmonte, U. Celano, J. Woo, S. Folkersma, C. Y. Chen, A. Redolfi, A. Fantini, R. Degraeve, S. Clima, W. Vandervorst, and M. Jurczak, in IEEE Symposium VLSI Technology (2016).
[11]A. Belmonte, W. Kim, B. T. Chan, N. Heylen, A. Fantini, M. Houssa, S. Member, M. Jurczak, and L. Goux, IEEE Trans. Electron Devices **60**, 3690 (2013).
[12]A. C. Torrezan, J. P. Strachan, G. Medeiros-Ribeiro, and R. S. Williams, Nanotechnology **22**, 485203 (2011).
[13]K. Zhang, K. Sun, F. Wang, Y. Han, Z. Jiang, J. Zhao, B. Wang, H. Zhang, X. Jian, and H. S. P. Wong, IEEE Electron Device Lett. **36**, 1018 (2015).
[14]C.-H. Cheng, F.-S. Yeh, and A. Chin, Adv. Mater. **23**, 902 (2011).
[15]U. Celano, L. Goux, A. Belmonte, K. Opsomer, A. Franquet, A. Schulze, C. Detavernier, O. Richard, H. Bender, M. Jurczak, and W. Vandervorst, Nano Lett. **14**, 2401 (2014).
[16]U. Celano, L. Goux, R. Degraeve, A. Fantini, O. Richard, H. Bender, M. Jurczak, and W. Vandervorst, Nano Lett. **15**, 7970 (2015).
[17]H. Lv, X. Xu, H. Liu, R. Liu, Q. Liu, W. Banerjee, H. Sun, S. Long, L. Li, and M. Liu, Sci. Rep. **5**, 7764 (2015).
[18]W. A. Hubbard, A. Kerelsky, G. Jasmin, E. R. White, J. Lodico, M. Mecklenburg, and B. C. Regan, Nano Lett. **15**, 3983 (2015).
[19]Q. Liu, J. Sun, H. Lv, S. Long, K. Yin, N. Wan, Y. Li, L. Sun, and M. Liu, Adv. Mater. **24**, 1844 (2012).
[20]Y. Takahashi, M. Kudo, I. Fujiwara, M. Shimuta, K. Ohba, and M. Arita, in *IEEE International Memory Workshop* (2015), p. 85.
[21]F. Yuan, Z. Zhang, C. Liu, F. Zhou, H. M. Yau, W. Lu, X. Qiu, H.-S. P. Wong, J. Dai, and Y. Chai, ACS Nano **11**, 4097 (2017).
[22]Y. Zhou, K. S. Yew, D. S. Ang, T. Kawashima, M. K. Bera, H. Z. Zhang, and G. Bersuker, Appl. Phys. Lett. **107**, 072107 (2015).
[23]T. Kawashima, K. S. Yew, Y. Zhou, D. S. Ang, M. K. Bera, and H. Z. Zhang, IEEE Electron Device Lett. **36**, 748 (2015).
[24]D. S. Ang, T. Kawashima, Y. Zhou, K. S. Yew, M. K. Bera, and H. Z. Zhang, ECS Trans. **69**, 169 (2015).
[25]Y. Zhou, T. Kawashima, and D. S. Ang, IEEE J. Electron Devices Soc. **5**, 188 (2017).
[26]X. Li, C. H. Tung, and K. L. Pey, Appl. Phys. Lett. **107**, 072903 (2008).
[27]N. Raghavan, K. L. Pey, X. Wu, W. Liu, X. Li, M. Bosman, and T. Kauerauf, IEEE Electron Device Lett. **32**, 252 (2011).
[28]Y. R. Luo, *Comprehensive Handbook of Chemical Bond Energies* (CRC Press, Boca Raton, FL, 2007).
[29]B. Butcher, G. Bersuker, L. Vandelli, A. Padovani, L. Larcher, A. Kalantarian, R. Geer, and D. C. Gilmer, in *IEEE International Memory Workshop* (2015), p. 52.
[30]Y.-G. Jin and K. J. Chang, Phys. Rev. Lett. **86**, 1793 (2001).
[31]Z. Q. Liu, D. P. Leusink, W. M. Lü, X. Wang, X. P. Yang, K. Gopinadhan, Y. T. Lin, A. Annadi, Y. L. Zhao, A. Roy Barman, S. Dhar, Y. P. Feng, H. B. Su, G. Xiong, T. Venkatesan, and Ariando, Phys. Rev. B **84**, 165106 (2011).
[32]X. Luo, B. Wang, and Y. Zheng, J. Appl. Phys. **106**, 073711 (2009).
[33]M. Kudo, Y. Ohno, K. Hamada, M. Arita, and Y. Takahashi, ECS Trans. **58**, 19 (2013).
[34]K. Kinoshita, T. Yamasaki, S. Yura, T. Ohno, and S. Kishida, Adv. Sci. Technol. **95**, 91 (2014).
[35]H.-P. Loock, L. M. Beaty, and B. Simard, Phys. Rev. A **59**, 873 (1999).
[36]Z. Q. Liu, W. M. Lü, X. Wang, Z. Huang, A. Annadi, S. W. Zeng, T. Venkatesan, and Ariando, Phys. Rev. B **85**, 155114 (2012).
[37]Z. Q. Liu, W. M. Lü, S. L. Lim, X. P. Qiu, N. N. Bao, M. Motapothula, J. B. Yi, M. Yang, S. Dhar, T. Venkatesan, and Ariando, Phys. Rev. B **87**, 220405(R) (2013).